Published in final edited form as:
Chemistry. 2016 December 12; 22(50): 18027–18035. doi:10.1002/chem.201603675.

Luminescent Thermochromism of 2D Coordination Polymers Based on Copper(I) Halides with 4-Hydroxythiophenol

Javier Troyano[a], **Josefina Perles**[b], **Pilar Amo-Ochoa**[a], **Jose Ignacio Martínez**[c], **Maria Concepción Gimeno**[d], **Vanesa Fernández-Moreira**[d], **Félix Zamora**[a],[e],[f], and **Salomé Delgado**[a]

[a]Departamento de Química Inorgánica, Universidad Autónoma de Madrid, Madrid, 28049, Spain

[b]Laboratorio de Difracción de Rayos X de Monocristal, Servicio Interdepartamental de Investigación, Universidad Autónoma de Madrid, E-28049 Madrid, Spain

[c]ESISNA Group, Department of Surfaces, Coatings and Molecular Astrophysics, Institute of Material Science of Madrid (ICMM-CSIC), 28049 Madrid, Spain

[d]Departamento de Química Inorgánica, Instituto de Síntesis Química y Catálisis Homogénea (ISQCH), CSIC-Universidad de Zaragoza, 50009 Zaragoza, Spain

[e]Instituto Madrileño de Estudios Avanzados en Nanociencia (IMDEA Nanociencia), Cantoblanco, 28049 Madrid, Spain

[f]Condensed Matter Physics Center (IFIMAC), Universidad Autónoma de Madrid, E-28049 Madrid, Spain

Abstract

Solvothermal reactions between copper(I) halides and 4-mercaptophenol give rise to the formation of three coordination polymers with general formula $[Cu_3X(HT)_2]_n$ (X= Cl, **1**; Br, **2**; and I, **3**). The structures of these coordination polymers have been determined by X-ray diffraction at both room temperature and low temperature (110 K), showing a general shortening in Cu-S, Cu-X and Cu···Cu bond distances at low temperatures. **1** and **2** are isostructural consisting of layers in which the halogen ligands act as μ_3-bridges joining two Cu1 and one Cu2 atoms whereas in **3** the iodine ligands is as μ_4-mode but the layers are quasi-isostructural with **1** or **2**. These compounds show a reversible thermochromic luminescence, with strong orange emission for **1** and **2**, but weaker for **3** at room temperature, while upon cooling at 77 K **1** and **2** show stronger yellow as well as **3** displays stronger green emission. DFT calculations have been used to rationalise these observations. These results suggest a high potential for this novel and promising stimuli-responsive materials.

Keywords

Coordination Polymers; Luminescent Materials; Thermochromic Coordination Polymers; Multifunctional Materials; Stimuli-Responsive Materials

Europe PMC Funders Author Manuscripts

Introduction

Inside the increasing interest in coordination polymers (CPs) in recent years in particular those containing Cu(I) constitute a relevant class because of their versatile architectures and physico-chemical properties.[1] Among them, Cu(I) halides represent a versatile type of building blocks that have been successfully used for the synthesis of CPs in combination with different neutral ligands obtaining, by simply varying reaction conditions, extraordinary structural diversity[1] and large variety of photophysical properties.[2] From an industrial and economic point of view, the development of new systems based on Cu(I) is strongly motivated by the low toxicity, low cost and availability of copper compared to the use of noble metals and rare earths,[3] making Cu(I) compounds excellent candidates for optoelectronic materials. The possibility to control and tune the photoluminescence properties of materials is particularly attractive for practical applications like sensing, detection, memories and display devices. In this sense, cubane-like $Cu_4I_4L_4$ (L= organic ligand) clusters constitute an interesting class of luminophors that have been extensively studied, exhibiting luminescent thermochromism influenced by metallophilic interactions.[2, 4] On the other hand, organosulfur-containing ligands have demonstrated their potential as linkers in the synthesis of metal-organic networks showing interesting electrical and luminescence properties.[5] In particular, it has been observed that the incorporation of thiolate-S bridging ligands between adjacent transition-metal centers is highly desirable in terms of magnetic, electrical and optical properties. This is due to the fact that the metal orbital energies are better matched for sulfur, leading to a higher delocalization of the spin/charge density through the bridging atoms. Despite the fact that there are some examples of Cu(I) halide coordination polymers based on organosulfur ligands with luminescent properties,[6] those that show stimuli-responsive luminescent are less frequent, and are usually based in cubane-like Cu_4I_4 or rhombohedral Cu_2I_2 clusters.[7] In this work, we have studied the preparation and characterization of a series of coordination polymers based on the combination of copper(I) halides with 4-mercaptophenol. These new materials have shown interesting optical properties including thermochromic luminescence. DFT calculations have allowed to rationalize this findings.

Results and Discussion

Synthesis and structural characterization

Coordination polymers **1**-**3** were obtained as crystalline solids by reaction of the corresponding copper(I) halide with 4-mercaptophenol in a 3:2 ratio at 120 °C under solvothermal conditions (see the Experimental Section). Powder X-ray diffraction confirmed the purity of the compounds (Figures S1-3). The crystal structures of compounds **1, 2** and **3** were determined by single-crystal X-ray diffraction analysis at both 296 and 110 K (named as **1LT, 2LT, 3LT**, respectively) in order to analyse the potential effect of the low temperature in the solid state. Detailed information about the structural determination is collected in the supplementary information. In all of the compounds with general formula $[Cu_3X(HT)_2]_n$, the asymmetric unit contains one 4-hydroxythiophenolate ligand, coordinated by the sulphur atom, one half halogen atom and one and a half crystallographically different Cu(I) atoms (Figures S4-S9). Compounds **1**-**3** consist of layers

of the 2D coordination polymer (Figure 1). These layers are joined through hydrogen bonds between hydroxyl groups in the 4-hydroxythiophenolate ligands (Figure S10).

Compounds **1** and **2** crystallise in the orthorhombic *Pnma* space group, both at room temperature and at 110 K. The halogen ligand and the sulphur atom act as μ_3 bridges joining two Cu1 and one Cu2 atoms to form polymeric 2D layers parallel to the *ac* plane (Figure 1). The structures solved at 296 K (**1** and **2**) display slightly larger cell parameters than the ones solved at 110 K (**1LT** and **2LT**), but the main differences are found in the distances around the copper atoms in the inorganic layer. At lower temperatures, the copper coordination environments change (Figure 2 and Table S14), specially the environment of Cu1 atoms. The coordination environment around both Cu1 and Cu2 atoms in the structures solved at 296 K can be described as slightly distorted planar trigonal with distances and angles that fall within the expected range. However, in **1LT** and **2LT,** besides the decrease in Cu-S and Cu-X bond distances, there is a change in the coordination environment of Cu1, as two of them sharing the same coordinated halogen atom get closer to yield a Cu-Cu interaction. A search of the structures deposited in the CSD database looking for similar Cu_2XS_4 arrangements did not yield any results.

Compound **3**, although not strictly isostructural with the chlorine and bromine derivatives (as it crystallises in two different space groups, $Pnm2_1$ for **3** and $P2_12_12$ for **3LT**), displays analogous polymeric layers, and a very similar arrangement of the $[Cu_3I(HT)_2]_n$ sheets. In both the structures displayed by compound **3**, the sulphur atoms act as μ_3-bridges joining two Cu1 and one Cu2 atoms, while the iodine ligands present a μ_4 mode, bridging two Cu1 and two Cu2 atoms. The differences between room temperature (**3**) and low temperature (**3LT**) structures lie mainly in the reduction of most distances in the coordination environments. The coordination polyhedra of Cu1 and Cu2 at 296 and 110 K display the same geometry. But the rearrangement of the atoms in the layers, and also of the rings, in the low temperature structure leads to a loss of symmetry (Figure S11) that in turn yields the change in the space group and the orientation of the cell vectors.

In order to stablish the thermal stability of polymers **1**-**3**, thermogravimetric analysis (TGA) and differential scanning calorimetry (DSC) under N_2 atmosphere were carried out (Figures S15-16). The decomposition temperatures of **1**–**3** fall in the range of 250 and 350 °C and increases following the order Cl<Br<I. Compounds **1**-**3** show a weight loss of *ca.* 30–40 % which can be assigned to decomposition of the arylthiolate ligand and subsequent formation of copper(II) sulfide and copper halides. Similar thermal transformations have been reported for homoleptic copper(I) arylthiolates, $[Cu(SPhR)]_n$, with decomposition temperatures between 200 and 300 °C.[8] Differential scanning calorimetry (DSC) measurements show exothermic peaks between 270 and 350 °C, corresponding to the mass loss observed in the TGA curves.

Electrical conductivity

It has been previously reported that CPs based on Cu(I) with organosulfur ligands are especially suitable to produce electrical conductive materials.[6a, 8–9] Therefore, the structures of compounds **1**-**3** showing sulphur atoms bridging metal centres are materials of

potential interest in terms of electrical behaviour. Therefore, several single-crystals of these compounds has been measured using a two-probe method at 300 K (Figures S12-14).

Since compounds **1** and **2** are isostructural (see structural description), their electrical conductivity must be related with the halide, chloride for **1** and bromide for **2**, present in their structures. However, the conductivity value found for **1** (4×10^{-7} Scm^{-1}) is two orders of magnitude higher than for **2** (3.9×10^{-9} Scm^{-1}). This result as well as the larger Cu-Cu distances displayed for **1** (Table S14) to those observed for **2**, contrasts with the general trend observed in other CPs with halide bridged ligands, in which the electrical conductivity increases with the volume of the halide based on a more effective overlapping between the dz-metal and the pz-halide orbitals as well as with shorter metal-metal distances.[9b] A deeper analysis of distances and angles in **1** and **2** show that both polymers consists of a *zig-zag -S-Cu-S-* chain propagating along the 001 direction, with very similar Cu-S distances (2.216-2.226 Å) and similar *S-Cu-S* angles (126.76-133.83°). These chains are joined together by the halide acting as triple bridge, being the side chain built-up by *-Cu-X-Cu-S-Cu-X-* (Figure 2). The shortest Cu-X distances are 2.338 and 2.462 Å for compounds **1** and **2** respectively. Previous work allow us justify the conductivity values observed in compounds **1** and **2**, according to the degree of geometric distortion showing by metal atoms. In this case, the crystal structures of the **1** and **2** show two crystallographically independent copper atoms, both being coordinated to two sulphur atoms and a halide ligand, with distorted trigonal planar geometry coordination. To quantify the degree of geometric distortion, from the values of the angles formed by the metal centres, we have calculated the deviation thereof with respect to 120° and the distance between the metal centre and the plane formed by the donor atoms (S and Cl or Br) (Table 1). These values indicate that, in case of **2** the distortion of trigonal plane is higher leading to a less effective orbital overlapping between the copper and the donor atoms, in agreement with the decrease in the conductivity value.

For compound **3**, an electrical conductivity value of 2×10^{-7} Scm^{-1} was founded, which is close to the value obtained for **1**. This compound displays a different structure to those found in **1** and **2**. In this case, the iodine acts as a μ_4-bridging ligand that shows a distorted tetrahedral geometry and the copper centres display two different coordination geometries, trigonal and tetrahedral. Therefore, is not possible to relate the effect of the geometric distortion with the observed electrical conductivity. In this case, the presence of the bulkier halide with a more effective overlapping with d_z-metal orbitals, and the coordination of the iodine atom to four metal centres that extend the connectivity between copper atoms could favour the conductivity.

Luminescent properties

Photophysical properties of compounds based on metal ions with d^{10} electronic configuration have attracted considerable attention.[2b, 4c, 10] Complexes based on Cu(I) are attractive because they display great structural diversity and may also show brightly luminescent even at room temperature.[1, 11]

The series of $[Cu_3X(HT)_2]$ (X= Cl, **1**; Br, **2**; I, **3**) have shown photoluminescence in solid state with strong orange emission for **1** and **2** and weaker for **3** upon excitation with a UV lamp (λ_{exc} = 365 nm). The quantum yields were measured in the solid state with values of 2.2 % for **1**, 2.6 % for **2** and a negligible value for **3**, whereas by grinding the solid samples the quantum yields raised to 4.6 % for **1** and 3.9 % for **2**.

When crystalline samples of **1**-**3** were packed in glass vials , immersed in liquid nitrogen and exposed to the irradiation of the same UV lamp, their emission change from orange to yellow (**1**-**2**) and from non-emissive to green (**3**). These changes were distinguished by naked eye and recorded by a digital camera (Figure 4). Compounds **1**-**3** returned to their initial emission after they were warmed to room temperature. Room temperature normalized emission spectra of **1**-**3** coordination polymers were recorded in the steady state mode at 298 K and have shown almost identical spectra (Figure 5a). The emission observed for **1** and **2** shown a broad band with maximum centred at 658 and 660 and emission lifetimes of 14 μs and 17.4 μs, respectively. The microsecond time scale of both compounds are indicative of an emission arising from a triplet state. Compound **3** does not emit at room temperature, however, as the temperature decrease, a broad band is also observed, with maximum centred at 565 at 275 K (Figure 5b).

In order to check the possible presence of emission arising from the ligand, the free ligand 4-mercaptophenol (4-mp) was also investigated. It shows very weak emission in high energy region with maximum centred at 420 and 469 nm (Figure S17) that could be assigned to ligand-centred $\pi \rightarrow \pi^*$ transitions. However, these bands, that could be described as high energy (HE) transitions, are absent in the compounds. To get more insight into the nature of the observed thermochromism, the emission spectra for **1**-**3** were registered at variable temperature (from 300 to 110 K) (Figure 6). By lowering the temperature from room temperature to 110 K, for complex **1** the main emission remains with similar value in energy, whereas a shoulder to higher energies appears at 575 nm. For complex **2**, a progressive blue shift is observed from 660 nm to 613 nm. In the case of complex **3**, the variable temperature experiment shows that emission appears at 250 K, centred at 565 nm, and is progressively displaced in energy to 544 nm at 110 K. Compound **1** shows emission lifetimes of 140 μs and 66 μs, respectively, for the two lower and higher energy bands, and for complexes **2** and **3** the lifetimes are 163.7 μs and 32 μs, respectively. This microsecond time scale is also indicative of an emission arising from a triplet state. Upon cooling, the increase observed for all compounds in the emission lifetimes could be attributed to the increase in structural rigidity in agreement with the low temperature structures, also indicating a decrease of the non-radiative rate constant. The thermochromic luminescence has been widely studied in cubane-like $[Cu_4I_4L_4]$ (L = organic ligand) clusters.[2b, 12] In all of them, a dual emission is observed. A high energy emission band at around 400-450 nm, which is dominant at low temperature and is assigned to a halogen-to-ligand charge transfer (^{3}XLCT) transition state and a low energy emission band at around 550-650 nm, dominant at room temperature, which is assigned as a cluster-centred excited state (^{3}CC).[2b, 13] DFT calculations recently reported[4a] allowed to assign that the low energy emission is due to a combination of a halide-to-copper charge transfer transition (XMCT) and of a copper-centred transition ($3d^{10} \rightarrow 3d^9 4s^1$ Cu, that is, CC*, which is essentially independent of the nature of the ligand (but

not the Cu···Cu distance) and the high-energy emission is assigned to ^{3}XLCT/^{3}MLCT mixed transition. Together with this structural type, for CuI-sulfide coordination polymers, the more common structure is single CuI stair step polymers, containing Cu_2I_2 rhomboid dimmers units with perpendicular sulphur-donor ligands or rhomboid dimmers linked into networks by monosulfide ligands in which a single sulphur atom acts as the bridge[7e] As far as we know, the 2D coordination polymers $[Cu_3X(HT)_2]$ (X= Cl, **1**; Br, **2**; I, **3**) described in this work represent a new structural type where the thermochromic luminescence phenomenon is observed. In order to get more insight into the nature of the origin of this thermochromism, the crystal structures for **1**-**3** were determined by single-crystal X-ray diffraction analysis at 110 K. In all compounds a slightly decreasing of cell parameters is observed; together with that, as we previously described in the structural description, at lower temperature, for isostructural **1**-**2** compounds, the copper coordination environments change, especially for Cu_1 atom (Figure 2) and shortening in Cu·····Cu interactions are observed (Δ = 0.022 nm and 0.014 nm for Cu_1 –Cu_1 and Cu_1 –Cu_2 distances respectively). These shortenings in the unit cell parameter and in the Cu···Cu distances could be associated with an increase in the medium rigidity; as the temperature decrease, the bonding character increases, and thus the energy levels are lowered. These structural changes are more significant for **3**; in this case, a phase transition takes place, changing from spatial group $Pmn2_1$ (at room temperature) to spatial group $P2_12_12$ (at 110 K) and leading a higher shortening in the Cu_1 –Cu_2 distances (Δ = 0.064 nm). This interesting phase transition is reversibly temperature dependent. As we can see, the origin of thermochromic luminescence in **1**-**3** is quite different to that reported for cubane $Cu_4I_4L_4$ cluster based compounds where two emission bands, low energy and high energy (LE and HE respectively) are observed. The emission behaviour in these compounds is different, because the high energy bands (HE) are not observed and only low energy bands (LE) take place. Based on precedent studies, the LE transitions may be attributed to ^{3}CC behaviour, and this ^{3}CC transition is itself a combination of halide-to-metal charge transfer (^{3}XMCT) and metal-centred transfer (^{3}MC: $3d^{10}\rightarrow 3d^9 4s^1$Cu) and the thermochromic luminescence is due to a significant change in Cu····· Cu distances in this ^{3}CC excitation state with temperature.[2b, 4a, 4c, 14] Due to the halide-to-metal charge transfer (^{3}XMCT) is less sensitive to the contraction of the Cu···Cu distances occurring when the temperature is decreased, we could conclude that the single emission band observed at lower temperature can be assigned as mainly originating from metal-centred transfer (^{3}MC; d^{10}Cu → d^9s^1Cu). For **3** the colour change with temperature is higher due to the transition of the room temperature phase to the low temperature phase (110 K) resulting in higher shortening in the Cu_1-Cu_2 distances (Δ = 0.064 nm) than in **1**-**2**, where this phase transition not take place. In summary, it seems there are direct evidence that thermochromic luminescence of these compounds is caused by temperature-dependent Cu···Cu distances and these Cu−Cu interactions are the key parameters that influence the luminescence properties of the ^{3}CC transition.

Theoretical calculations

In Figure 7a, we show the computed Quasi-particle GW+BSE-corrected DFT band-structure diagrams of all the compounds **1**, **2**, **3** and **3LT** along a most relevant symmetry line Γ→Z→ZY (being the ΓZ direction along the monodimensional chains axis). From these band-structure diagrams we can extract some valuable information. On one side, it is

important to remark that the band-structure morphology is quite similar for all the compounds, yielding electronic gaps at Γ-point of 2.16 and 2.24 eV for **1** and **2**, and 1.87 and 1.63 eV for **3** and **3LT**, respectively. These moderately high values of the transport gaps reveal that all the compounds behave as wide-gap semiconductors, which perfectly agrees with the experimental low values obtained for the electrical conductivities. On the other hand, the comparison between the band-diagrams for the **3** and **3LT** cases shows a reduction of the gap from *LT* to *RT* conditions of around 0.25 eV, as well as a noticeable shift toward lower energies of both the conduction band (CB) and the subsequent upper state in energy (named as CB+1), which breaks its degeneracy w.r.t. the **3LT** case. This behaviour should have a significant effect in the excitation spectrum (see below). Figure 7b shows the 3D orbital isodensities (all of them computed with a value of 10^{-4} $e^{-}Å^{-3}$) for the compounds **1**, **2** and **3LT** for their valence and conduction bands (VB and CB), and for the energetically lower and upper bands (VB-1 and CB+1). For all the cases it is possible to appreciate a similar spatial distribution morphology: VB-1 and VB are composed of atomic contributions mostly located onto the metal chains, whereas the CB and CB+1 are composed of atomic contributions tending to be located mostly on the external ligands. Consequently, VB-1/VB→CB/CB+1 leads to the expected chain/ligands transitions as the lowest energy electronic transitions.

Figure 7a shows the experimental spectra measured in solid state of all the compounds. At *LT* these spectra show prominent peaks located at around 658, 575; 613 and 544 nm for the compounds **1**, **2** and **3** respectively. In particular, at *LT* compound **1** exhibits a two-peak structure formed by a less intense peak located at around 575 nm that tends to vanish with the increasing temperature and a primary peak located at around 658 nm. Interestingly, for all the cases these prominent peaks show a slight broadening and a shift toward higher wavelengths as the temperature increases. In the attempt to rationalize the excitations involved in the *LT* experimental spectra of all the compounds we have carried out (as explained above) DFT-based calculations of their many-body excitation spectra. For that purpose, we have computed the oscillator strengths of the major transitions contributing to the excitation spectra at that wavelength range, resulting those corresponding to VB-1/VB→CB/CB+1. In Table 2 we show the oscillator strengths (in a.u.) for those four transitions for all the **1**, **2** and **3** compounds at *LT* conditions, and for **3** at *RT*. Regarding the values of the Table 2, for the three first cases we conclude that the most important transitions are the VB-1→CB+1 and the VB→CB+1, with values of 0.1032 and 0.1847 a.u. at 556.3 and 581.1 nm, respectively for **1** (to be compared with the experimental threshold value of 575 nm), 0.1438 and 0.2742 a.u. at 543.5 and 572.7 nm, respectively for **2** (to be compared with the experimental threshold value of 615 nm), and 0.1132 and 0.2247 a.u. at 522.3 and 531.7 nm, respectively for **3** (to be compared with the experimental threshold value of 545 nm). In order to mimic the experimental spectral resolution, on the basis of these excitations we have constructed the excitation spectra for the different compounds by assigning a Lorentzian broadening of 500 cm^{-1} to each one of the four contributing excitations.

As we can observe, the comparison between the experimental and the computed spectra is quite reasonable, even capturing some of the ordering in wavelength of the most pronounced peaks for the different systems at *LT* conditions.

Additionally, for the *RT* compound **3**, with a structural transition experimentally evinced, we have computed the excitation spectrum in the same way. For this case, as commented, the noticeable shift toward lower energies of both the CB and CB+1 (which breaks its degeneracy), has its reflection in the excitation oscillator-strengths and wavelengths obtaining for VB-1→CB+1 and VB→CB+1, values of 0.1465 and 0.1041 a.u. at 548.4 and 597.1 nm, respectively.

The spectrum constructed from these excitations reveals, indeed, the observed shift toward higher wavelengths and the appearance of a secondary shoulder-peak above 600 nm, which is also visible in the experimental spectrum for **3** at *RT* conditions. This may be explained in terms of the effect that the structural transition has in the electronic features of the compound **3**, where the reduction of the gap and the splitting of the band CB+1 towards lower energies induce the appearance of the secondary features in the excitation spectrum. This is also noticeable for the rest of the spectra at higher temperatures than *LT*. Unfortunately; this effect has been only computed for the compound **3** for which the structural transition is observed by X-ray diffraction. Additionally, we have computed the CI-NEB transition energy barrier between the compounds **3** and **3LT**, obtaining a value of ΔE_{TS}=0.08 eV, which justifies from a theoretical point of view the structural transition for **3** from *LT* to *RT* conditions.

Conclusions

Three new 2D coordination polymers with general formula $[Cu_3X(HT)_2]_n$ (X= Cl, **1**; Br, **2**; I, **3**) have been synthesized by solvothermal reactions between copper(I) halides and 4-mercaptophenol. While **1** and **2** are isostructural, **3** shows slight differences since the iodine act as μ_4-bridging ligands while in **1** and **2** the halides coordinate as μ_3-bridging ligands. The three structures shows Cu_2XS_4 arrangements that represent a new structural motifs for copper(I) coordination polymers. Their electrical properties have been studied, showing moderate conductivity values of 4×10^{-7}, 3.9×10^{-9} and 2×10^{-7} Scm^{-1} for **1**-**3** respectively. These values can be rationalized based on a detailed structural analysis of distances and angles that affect to the metal-ligand orbitals overlapping along the coordination sheets, and agree with the calculated electronic gaps. Interestingly, the study of their luminescent properties show reversible thermochromic luminescence, with strong orange emission for compounds **1** and **2** and weaker for **3** at room temperature and changes to stronger yellow (**1**-**2**) and green (**3**) emission upon cooling at 77 K. To get more insight into the nature of the observed thermochromism, variable temperature experiments have been carried out and theirs structure were also solved at 110 K. The results obtained seems to indicate that there are direct evidence that luminescent thermochromism of these compounds is caused by temperature-dependent Cu···Cu distances and these Cu−Cu interactions are the key parameters that influence the luminescent properties. According with this, the higher color change with temperature observed for **3** is due to the structural transition that takes place of the room temperature to the low temperature (110 K), resulting in higher shortening in the Cu_1–Cu_2 distances than in **1**-**2**. This is supported by DFT-based calculations, where the comparison between the experimental and the computed spectra is quite reasonable.

Europe PMC Funders Author Manuscripts

In summary, these news compounds represent a series of novel interesting multifunctional two-dimensional coordination polymers showing moderate electrical conductivity but a significant reversible luminescent thermochromism.

Experimental Section

Materials and Methods

All the reagents were purchased from Sigma-Aldrich and used as received. FTIR spectra (KBr pellets) were recorded on a Perkin-Elmer 1650 spectrophotometer. C, H, N, S elemental analyses were performed by the Microanalysis Service of the Universidad Autónoma de Madrid on a Perkin-Elmer 240 B microanalyser. Powder X-ray diffraction experiments were carried out on a Diffractometer PANalyticalX'Pert PRO theta/2theta primary monochromator and detector with fast X'Celerator. The samples have been analysed with scanning theta/2theta. Direct current (DC) electrical conductivity measurements were performed on different single crystals of compounds **1**-**3** between two carbon paint contacts. The samples were measured at 300 K applying an electrical current with voltages form +10 to -10 V. Steady-state photoluminescence spectra were recorded with a Jobin-Yvon Horiba Fluorolog FL-3-11 spectrometer using band pathways of 3 nm for both excitation and emission. Phosphorescence lifetimes were recorded with an IBH 5000F coaxial nanosecond flashlamp. Fluorescent lifetimes with a Data station HUB-B with a nanoLED controller and DAS6 software. The lifetime data were fitted with the Jobin-Yvon software package. Measurements at variable temperature were done with an Oxford Cryostat Optistat DN. The lifetime data were fitted using the Jobin-Yvon IBH software DAS6 v6.1. The quantum yields were measured in a Hamamatsu Photonics KK in solid. Computational Details. In order to rationalize the experimental photoemission results obtained for the different compounds, we have carried out first-principles DFT-based calculations of the many-body excitation spectra for the **1**-**3** $[Cu_3X(HT)_2]_n$ polymers. For that purpose we have applied many-body perturbation theory via the Quasi-particle approximation GW correction[15] to conventional DFT, combined to the Bethe–Salpeter equation (BSE)[16] as follows: i) first, the ground-state electronic structure of the different polymers was obtained with the QUANTUM ESPRESSO code[17] by using an LDA XC–functional[18] and norm-conserving pseudopotentials;[19] ii) second, electronic quasi-particle corrections were calculated within the GW approximation to the XC self-energy;[15] and iii) finally, the BSE was solved for coupled electron-hole excitations[20] thereby accounting for the screened electron-hole attraction and the unscreened electron-hole exchange. Steps ii) and iii) were performed with the YAMBO simulation package[21]. The GW+BSE formalism: i) accounts, by construction, for excitonic effects, which turn into significant in highly correlated systems; ii) combines the excellent performance of the GW+LDA on the ground-state electronic structure calculations with the high accuracy of the BSE for the calculation of excitations; and iii) it is able to distinguish the response to each individual light-polarization component for each particular excitation. In all the simulations we have used the structures obtained by X-ray diffraction. For all the polymers, the residual forces acting on each atom in all the calculations were below 0.1 eV/Å, which is low enough to guarantee perfectly converged and realistic results for such complex systems from a computational point of view. Besides, a structural transition for the $[Cu_3I(HT)_2]_n$ compound has been

experimentally evinced from low temperature (*LT*) to *RT* conditions. To obtain the transition-state energy barrier between both structural configurations we have used the CI-NEB approach,[22] implemented within the QUANTUM ESPRESSO package,[17] where the initial, the final, and 12 intermediate image-states were free to fully relax.

Single Crystal X-ray Data Collection and Structure Determination. The X-ray diffraction data collections and were done at 296(2) K and 100(2) K on a Bruker Kappa Apex II diffractometer using graphite-monochromated Mo-Kα radiation (λ=0.71073 Å). The cell parameters were determined and refined by a least-squares fit of all reflections. A semi-empirical absorption correction (SADABS) was applied for all cases. All the structures were solved by direct methods and refined by full-matrix least-squares on F2 including all reflections (SHELXL97).[23] Relevant data acquisition and refinement parameters are gathered in Tables S1-S6. Crystal structured have been deposited at the CSD with deposition numbers CCDC 1491209-1491214. Compound **3** crystallised in perfect inversion twins, and although many attempts were made to select an untwinned single crystal, structures **3** and **3LT** had to be solved from one of the two-domain inversion twins.

Synthesis of $[Cu_3Cl(HT)_2]_n$ (1)

A solution of 4-mercaptophenol (130 mg, 1.00 mmol) in EtOH (10 mL) was mixed with CuCl (150 mg, 1.50 mmol) in 5 mL of CH_3CN and the mixture was sealed in a 23 mL Teflon-lined stainless steel autoclave. The reactor was heated at 120 °C for 20 h followed by slow cooling to room temperature. Bright yellow block crystals of **1** were obtained, washed with CH_3CN and Et_2O, and dried on air (96 mg, 40% yield based on Cu). Anal. Calcd (%) for $C_{12}H_{10}ClCu_3O_2S_2$: C, 30.25; H, 2.12; S, 13.46. Found (%): C, 30.17; H, 2.25; S, 13.24. IR (KBr, cm^{-1}): 3160 (w), 1581 (m), 1490 (m), 1456 (s), 1436 (s), 1376 (m), 1280 (w), 1228 (s), 1159 (s), 1085 (s), 1009 (s), 825 (s), 811 (s), 632 (w).

Synthesis of $[Cu_3Br(HT)_2]_n$ (2)

The compound was synthesized as described for **1**, except using CuBr (219 mg, 1.50 mmol). Yellow block crystals of **2** were obtained (111 mg, 43% yield based on Cu). Anal. Calcd (%) for $C_{12}H_{10}BrCu_3O_2S_2$: C, 27.67; H, 1.94; S, 12.31. Found (%): C, 27.21; H, 2.12; S, 12.19. IR (KBr, cm^{-1}): 3168 (w), 1581 (m), 1488 (s), 1444 (s), 1374 (m), 1280 (w), 1228 (s), 1159 (m), 1085 (m), 1009 (m), 824 (s), 810 (s), 632 (w).

Synthesis of $[Cu_3I(HT)_2]_n$ (3)

The compound was synthesized as described for **1**, except using CuI (291 mg, 1.50 mmol). A pale yellow powder was obtained (87 mg, 31% yield based on Cu). Anal. Calcd (%) for $C_{12}H_{10}ICu_3O_2S_2$: C, 25.38; H, 1.77; S, 11.29. Found (%): C, 24.82; H, 1.89; S, 10.77. IR (KBr, cm^{-1}): 3158 (w), 1584 (s), 1491 (m), 1469 (s), 1379 (m), 1237 (s), 1161 (m), 1097 (m), 1085 (m), 1009 (m), 815 (s), 807 (s), 632 (m). Bright yellow crystals of **3** suitable for single-crystal X-ray diffraction were obtained by using an excess of CuI (240 mg, 1.25 mmol) with 4-mercaptophenol (65 mg, 0.50 mmol) in 15 mL of a EtOH:CH_3CN mixture (2:1 in volume). The reactor was heated at 120 °C for 48 h and then slowly cooled down to room temperature at a rate of 5 °C per hour.

Supplementary Material

Refer to Web version on PubMed Central for supplementary material.

Acknowledgements

This work was supported by MICINN (MAT2013-46753-C2-1-P). JIM acknowledges funding from the ERC-Synergy Program (Grant ERC-2013-SYG-610256 NANOCOSMOS) and computing resources from CTI-CSIC.

References

[1]. Peng R, Li M, Li D. Coord Chem Rev. 2010; 254:1–18.

[2]. a) Barbieri A, Accorsi G, Armaroli N. Chem Commun. 2008:2185–2193.b) Ford PC, Cariati E, Bourassa J. Chem Rev. 1999; 99:3625–3648. [PubMed: 11849032] c) Wing-Wah Yam V, Kam-Wing Lo K. Chem Soc Rev. 1999; 28:323–334.

[3]. Yang X, Jones RA, Huang S. Coord Chem Rev. 2014; 273–274:63–75.

[4]. a) Perruchas S, Tard C, Le Goff XF, Fargues A, Garcia A, Kahlal S, Saillard J-Y, Gacoin T, Boilot J-P. Inorg Chem. 2011; 50:10682–10692. [PubMed: 21957984] b) Li S-L, Zhang F-Q, Zhang X-M. Chem Commun. 2015; 51:8062–8065.c) Vitale M, Ford PC. Coord Chem Rev. 2001; 219-221:3–16.

[5]. Zhu H-B, Gou S-H. Coord Chem Rev. 2011; 255:318–338.

[6]. a) Delgado S, Sanz Miguel PJ, Priego JL, Jiménez-Aparicio R, Gómez-García CJ, Zamora F. Inorg Chem. 2008; 47:9128–9130. [PubMed: 18817369] b) Gallego A, Castillo O, Gómez-García CJ, Zamora F, Delgado S. Inorg Chem. 2012; 51:718–727. [PubMed: 22148743] c) Troyano J, Perles J, Amo-Ochoa P, Martinez JI, Zamora F, Delgado S. CrystEngComm. 2014; 16:8224–8231.d) Troyano J, Perles J, Amo-Ochoa P, Zamora F, Delgado S. CrystEngComm. 2016; 18:1809–1817.

[7]. a) Knorr M, Khatyr A, Dini Aleo A, El Yaagoubi A, Strohmann C, Kubicki MM, Rousselin Y, Aly SM, Fortin D, Lapprand A, Harvey PD. Crys Grow Des. 2014; 14:5373–5387.b) Kim TH, Shin YW, Jung JH, Kim JS, Kim J. Angew Chem Int Ed. 2008; 47:685–688.c) Bonnot A, Knorr M, Guyon F, Kubicki MM, Rousselin Y, Strohmann C, Fortin D, Harvey PD. Crys Grow Des. 2016; 16:774–788.d) Knorr M, Pam A, Khatyr A, Strohmann C, Kubicki MM, Rousselin Y, Aly SM, Fortin D, Harvey PD. Inorg Chem. 2010; 49:5834–5844. [PubMed: 20509605] e) Henline KM, Wang C, Pike RD, Ahern JC, Sousa B, Patterson HH, Kerr AT, Cahill CL. Crys Grow Des. 2014; 14:1449–1458.

[8]. Che C-M, Li C-H, Chui SS-Y, Roy VAL, Low K-H. Chem Eur J. 2008; 14:2965–2975. [PubMed: 18350558]

[9]. a) Huang X, Sheng P, Tu Z, Zhang F, Wang J, Geng H, Zou Y, Di C-a, Yi Y, Sun Y, Xu W, et al. Nat Commun. 2015; 6b) Givaja G, Amo-Ochoa P, Gomez-Garcia CJ, Zamora F. Chem Soc Rev. 2012; 41:115–147. [PubMed: 21713280] c) Low K-H, Roy VAL, Chui SS-Y, Chan SL-F, Che C-M. Chem Commun. 2010; 46:7328–7330.

[10]. Yam VW-W, Wong KM-C. Chem Commun. 2011; 47:11579–11592.

[11]. Tsuge K, Chishina Y, Hashiguchi H, Sasaki Y, Kato M, Ishizaka S, Kitamura N. Coord Chem Rev. 2016; 306(Part 2):636–651.

[12]. a) Ford PC, Vogler A. Acc Chem Res. 1993; 26:220–226.b) Ford PC. Coord Chem Rev. 1994; 132:129–140.

[13]. Perruchas S, Goff XFL, Maron S, Maurin I, Guillen F, Garcia A, Gacoin T, Boilot J-P. J Amer Chem Soc. 2010; 132:10967–10969. [PubMed: 20698644]

[14]. a) De Angelis F, Fantacci S, Sgamellotti A, Cariati E, Ugo R, Ford PC. Inorg Chem. 2006; 45:10576–10584. [PubMed: 17173412] b) Vega A, Saillard J-Y. Inorg Chem. 2004; 43:4012–4018. [PubMed: 15206883] c) Liu Z, Djurovich PI, Whited MT, Thompson ME. Inorg Chem. 2012; 51:230–236. [PubMed: 22133068]

[15]. Hybertsen MS, Louie SG. Phys Rev B. 1986; 34:5390–5413.

[16]. Onida G, Reining L, Rubio A. Rev Mod Phys. 2002; 74:601–659.

[17]. Paolo G, Stefano B, Nicola B, Matteo C, Roberto C, Carlo C, Davide C, Guido LC, Matteo C, Ismaila D, Andrea Dal C, et al. J Phys Cond Matt. 2009; 21:395502.

[18]. Perdew JP, Zunger A. Phys Rev B. 1981; 23:5048–5079.

[19]. Troullier N, Martins JL. Phys Rev B. 1991; 43:1993–2006.

[20]. a) Rohlfing M, Louie SG. Phys Rev Lett. 1999; 83:856–859.b) Benedict LX, Shirley EL, Bohn RB. Phys Rev Lett. 1998; 80:4514–4517.c) Albrecht S, Reining L, Del Sole R, Onida G. Phys Rev Lett. 1998; 80:4510–4513.

[21]. Marini A, Hogan C, Grüning M, Varsano D. Comp Phys Comm. 2009; 180:1392–1403.

[22]. Berne, GCBJ.; Coker, DF. Classical and Quantum Dynamics in Condensed Phase Simulations. WORLD SCIENTIFIC; 1998.

[23]. Sheldrick GM. Acta Crystallogr Sect A. 1990; 46:467.

Europe PMC Funders Author Manuscripts

Europe PMC Funders Author Manuscripts

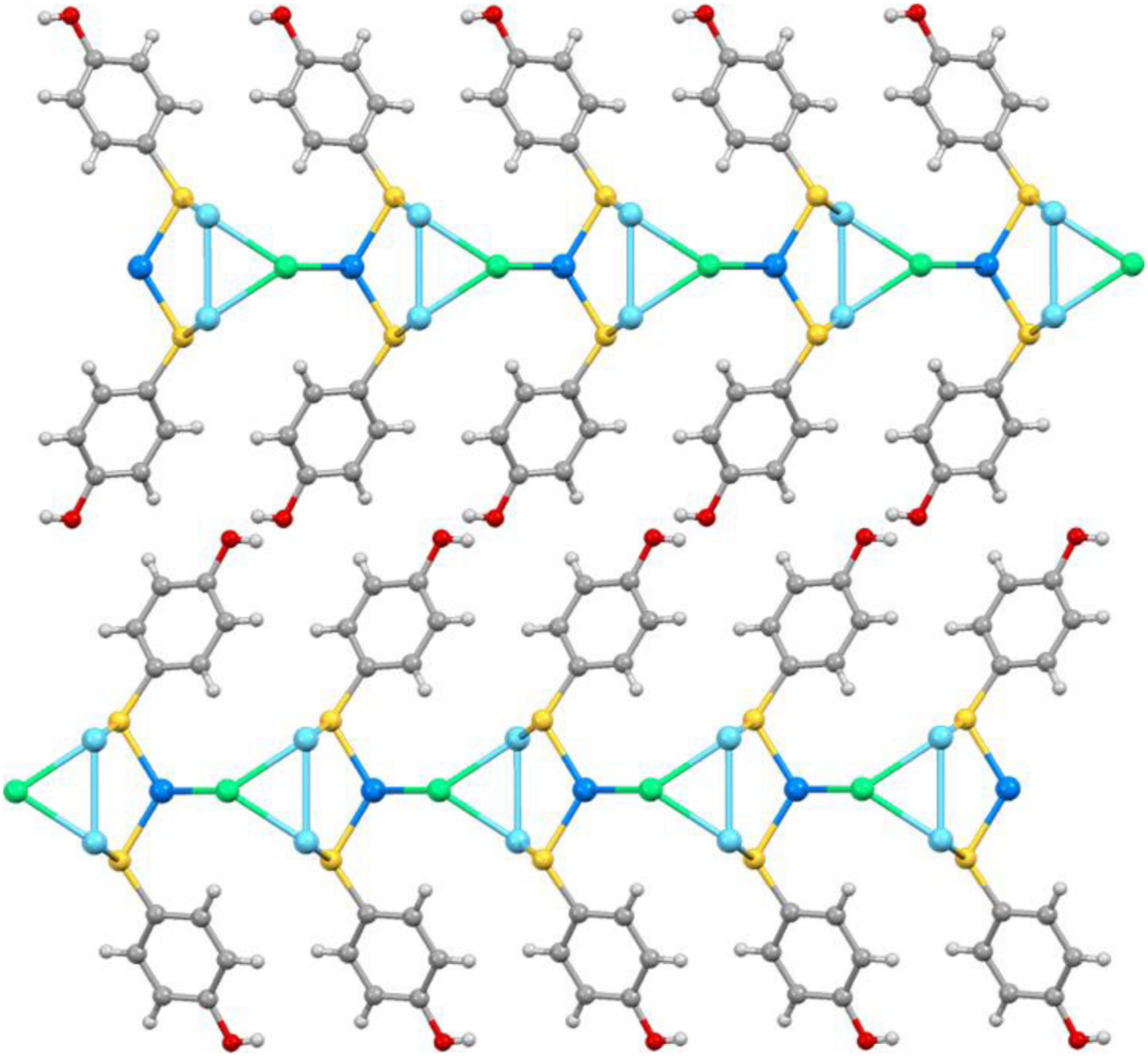

Figure 1.
Lateral view along the *c* axis of two adjacent layers in **1**. Crystallographically different copper atoms Cu1 and Cu2 are depicted in light blue and dark blue, respectively.

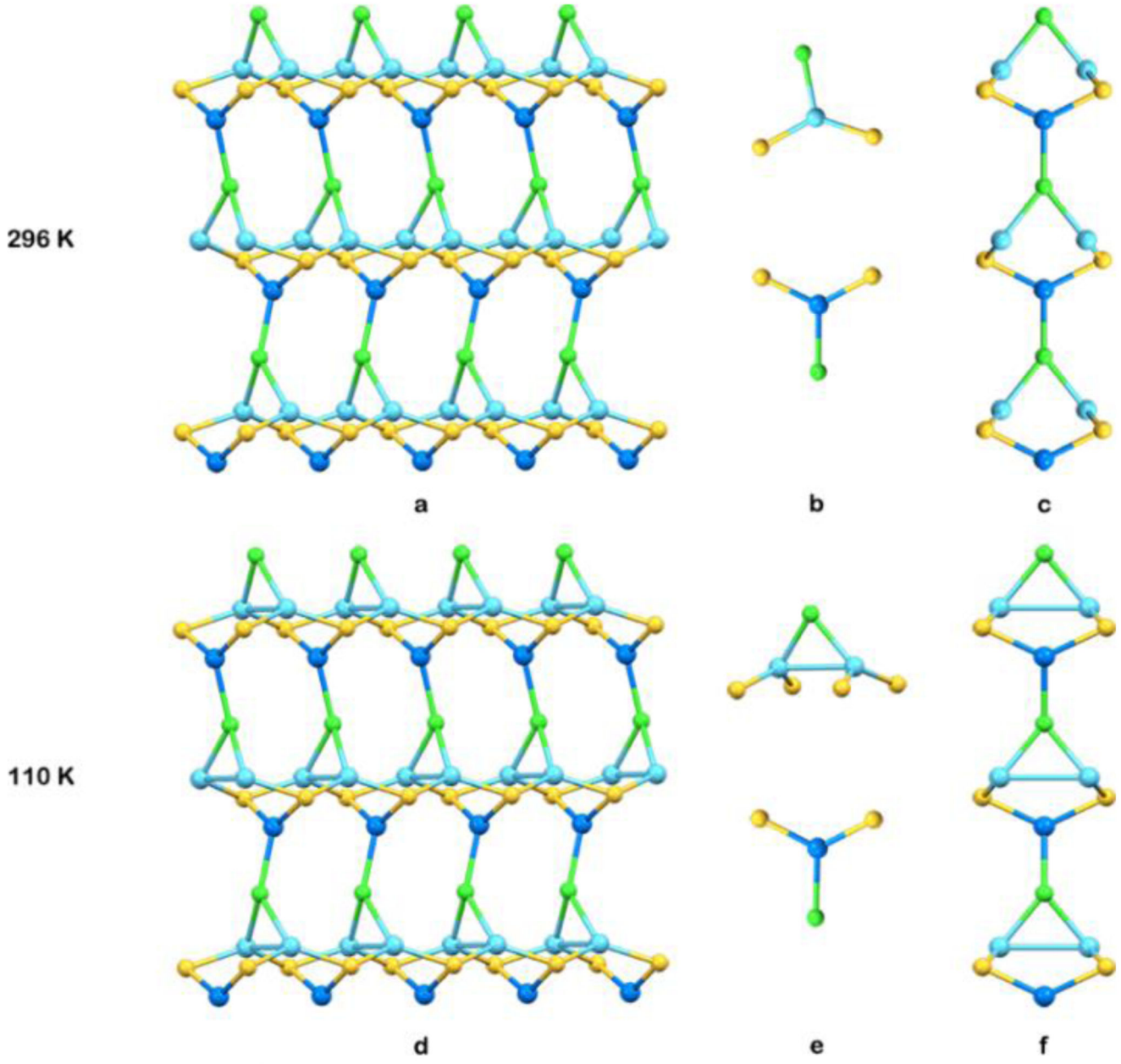

Figure 2.

View of the inorganic part of one layer in the structure of **1** at room temperature (**a**); coordination environments within the layer for copper atoms Cu1 (**b** top, in light blue) and Cu2 (**b** bottom, in dark blue); and lateral view of the layer along the *c* direction (**c**). Images **d**, **e** and **f** show analogous views in the structure solved at 110 K (**1LT**).

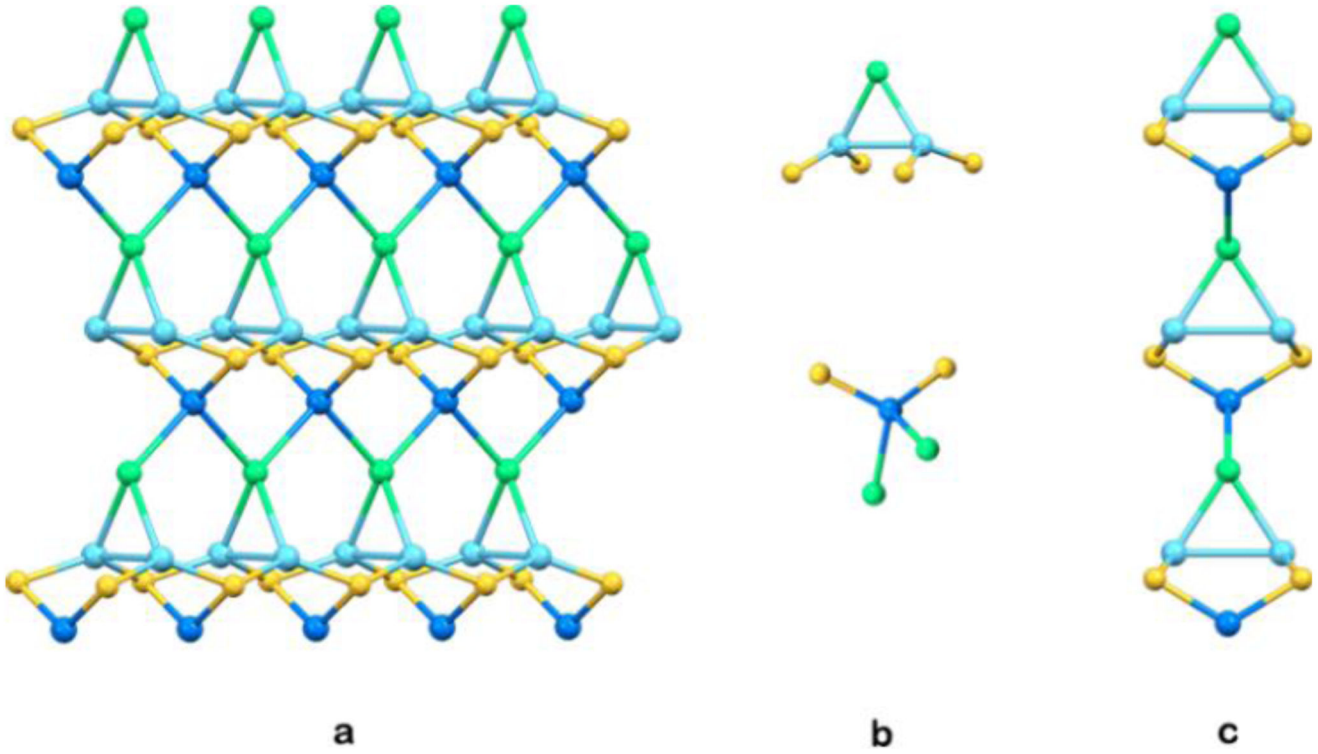

Figure 3.

View of the inorganic part of one layer in the structure of **3** (**a**), coordination environments of copper atoms Cu1 (**b** top, in light blue) and Cu2 (**b** bottom, in dark blue); and lateral view of the layer along the *a* direction (**c**).

Europe PMC Funders Author Manuscripts

Europe PMC Funders Author Manuscripts

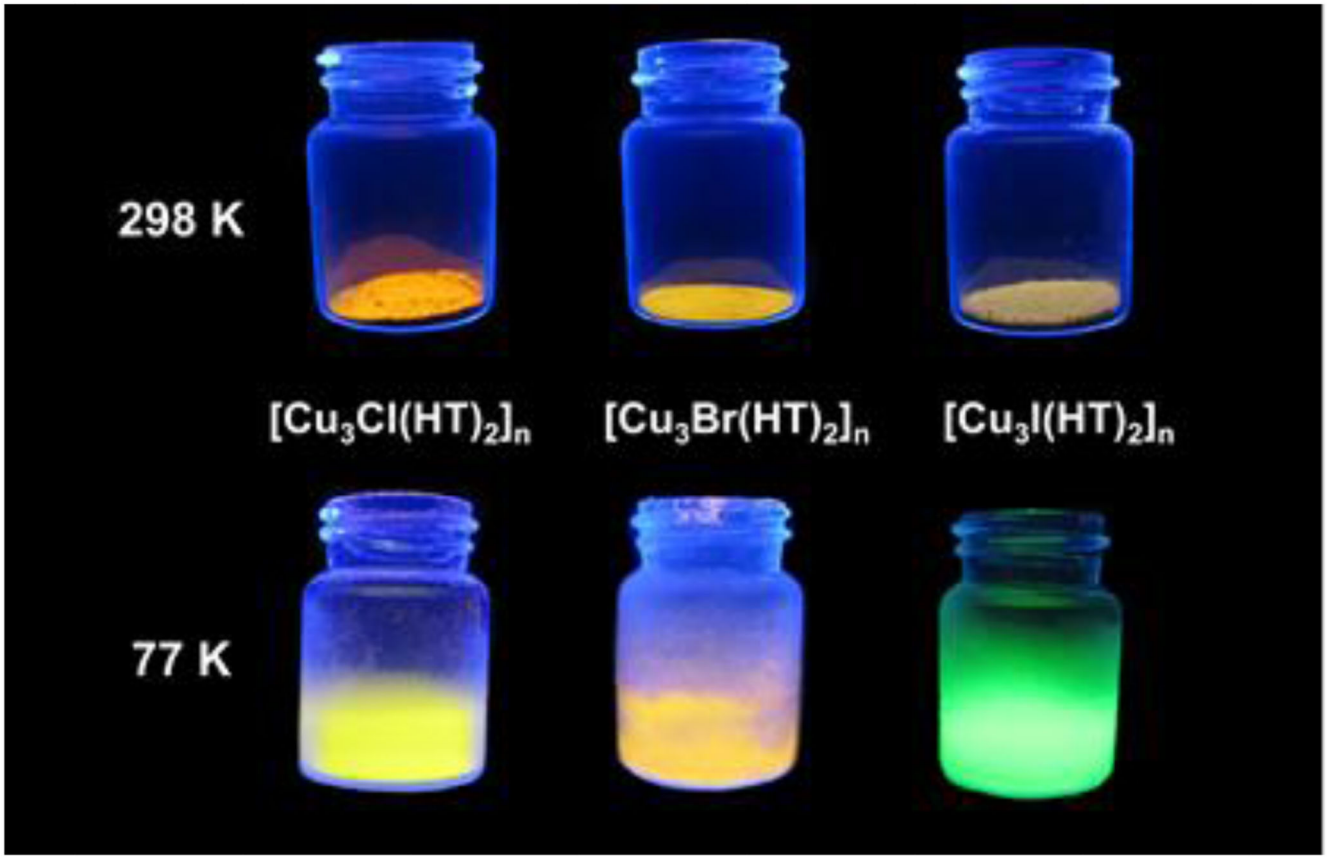

Figure 4.
Photographs of **1**-**3** as solid samples at 298 K and 77 K under the UV-lamp (λ = 365 nm).

Europe PMC Funders Author Manuscripts

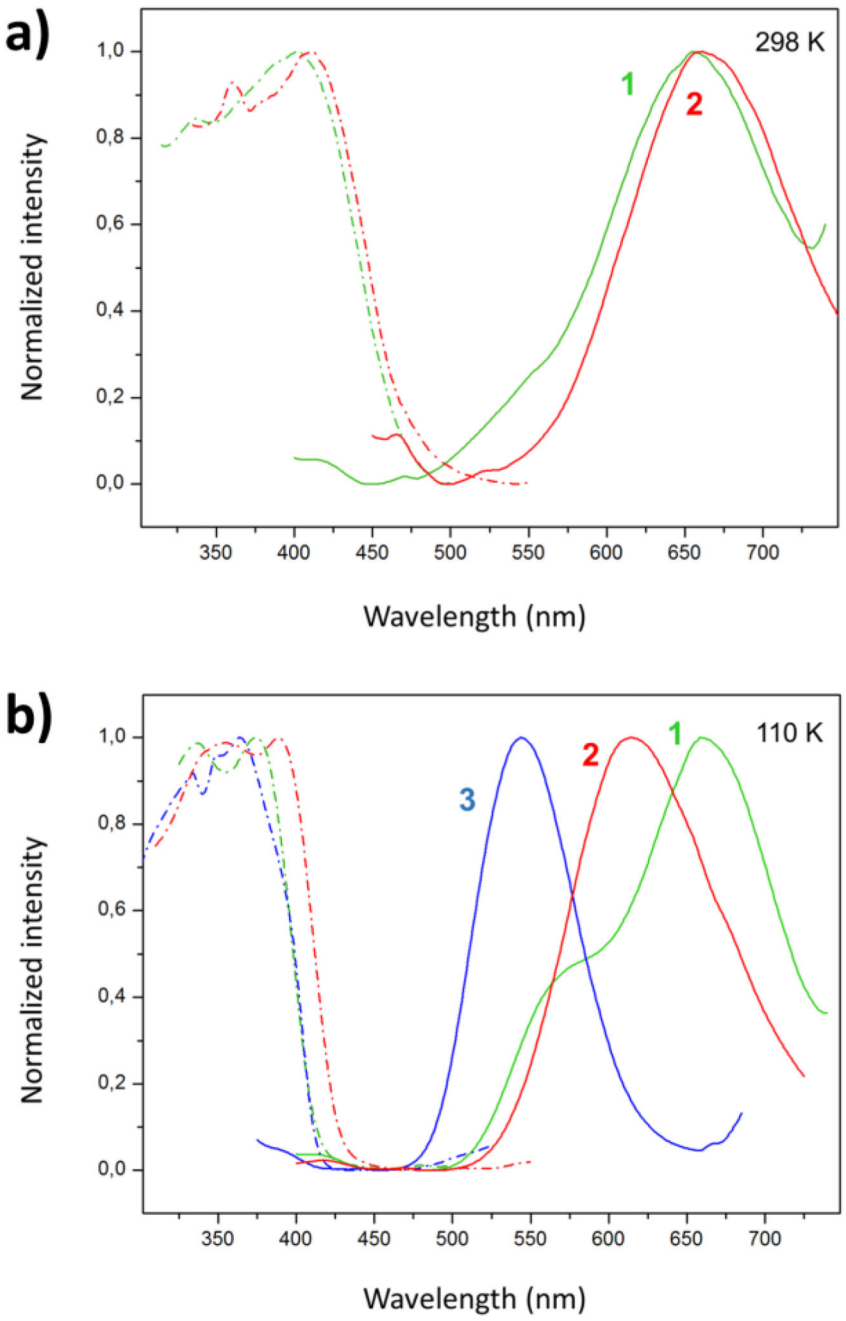

Figure 5.

Normalized excitation (dotted line) and emission (continuous line) spectra of **1** (green), **2** (red) and **3** (blue) at 298 (a) and 110 K (b).

Europe PMC Funders Author Manuscripts

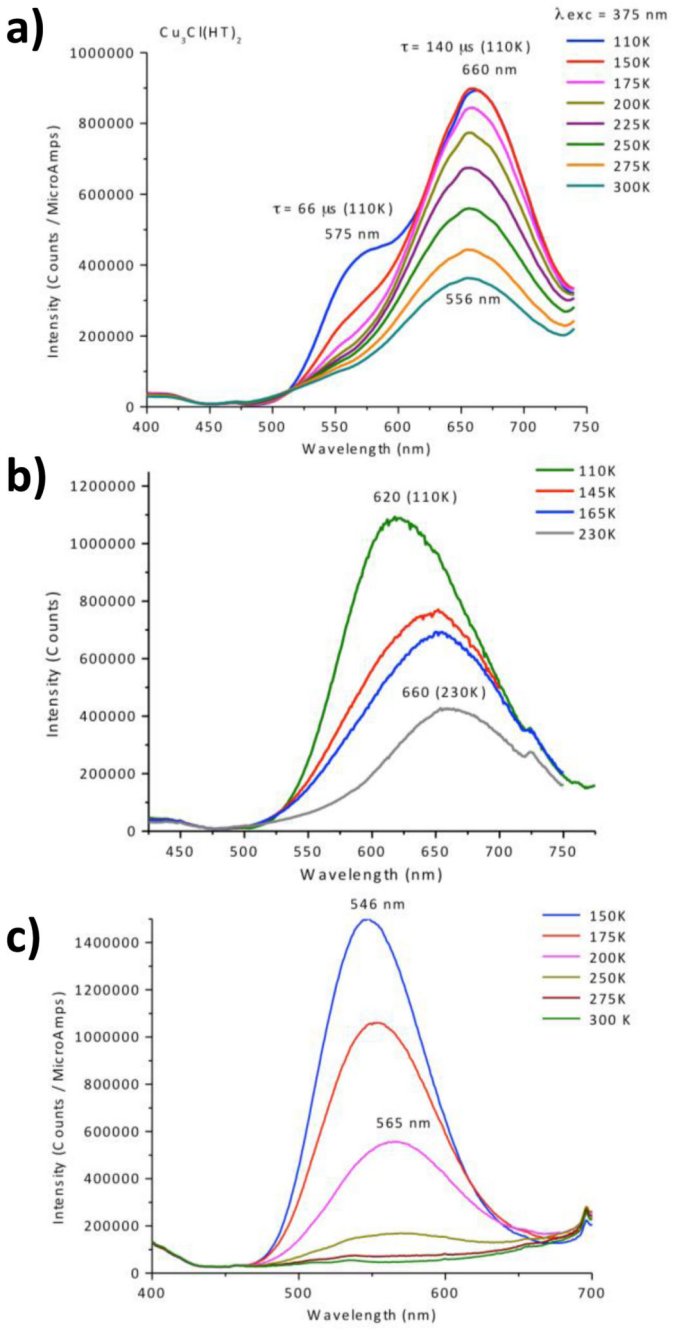

Figure 6.

Experimental photoemission spectra for the compounds **1** (a), **2** (b) and **3** (c) at different temperatures (λ_{exc} = 375 nm).

Europe PMC Funders Author Manuscripts

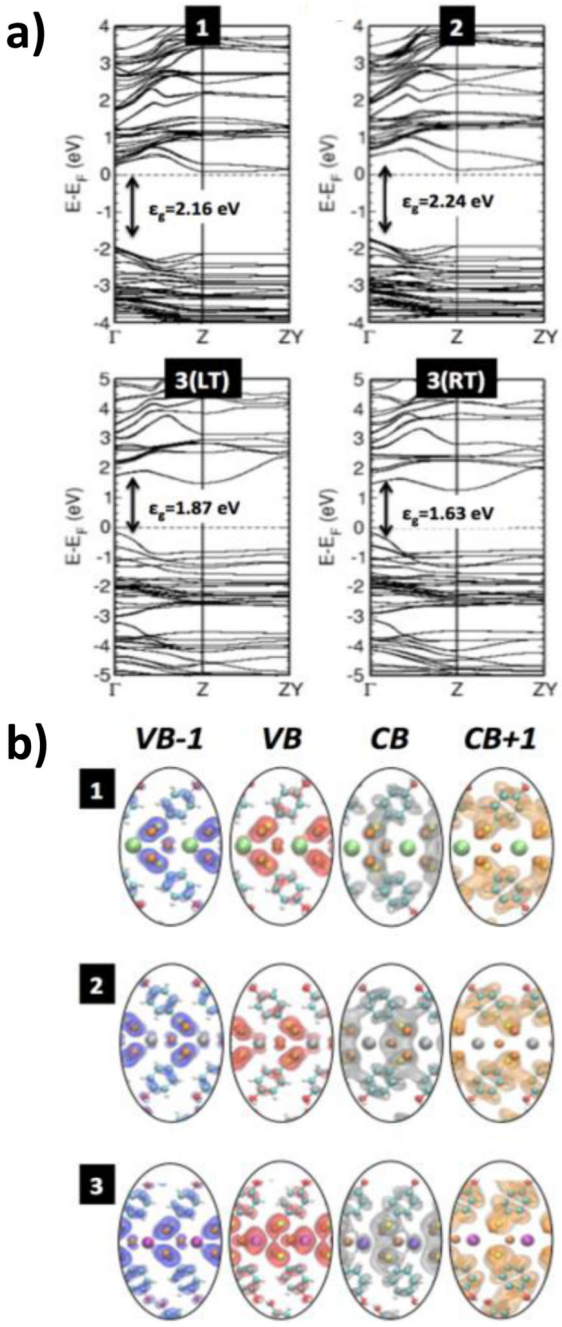

Figure 7.

a) Quasi-particle GW+BSE-corrected DFT band-structure diagrams for the compounds **1**, **2**, **3(LT)** and **3(RT)** along the symmetry line Γ→;Z→ZY. b) 3D orbital isodensities (10^{-4} $e^{-}Å^{-3}$) for **1**, **2** and **3(LT)** for VB-1, VB, CB and CB+1.

Europe PMC Funders Author Manuscripts

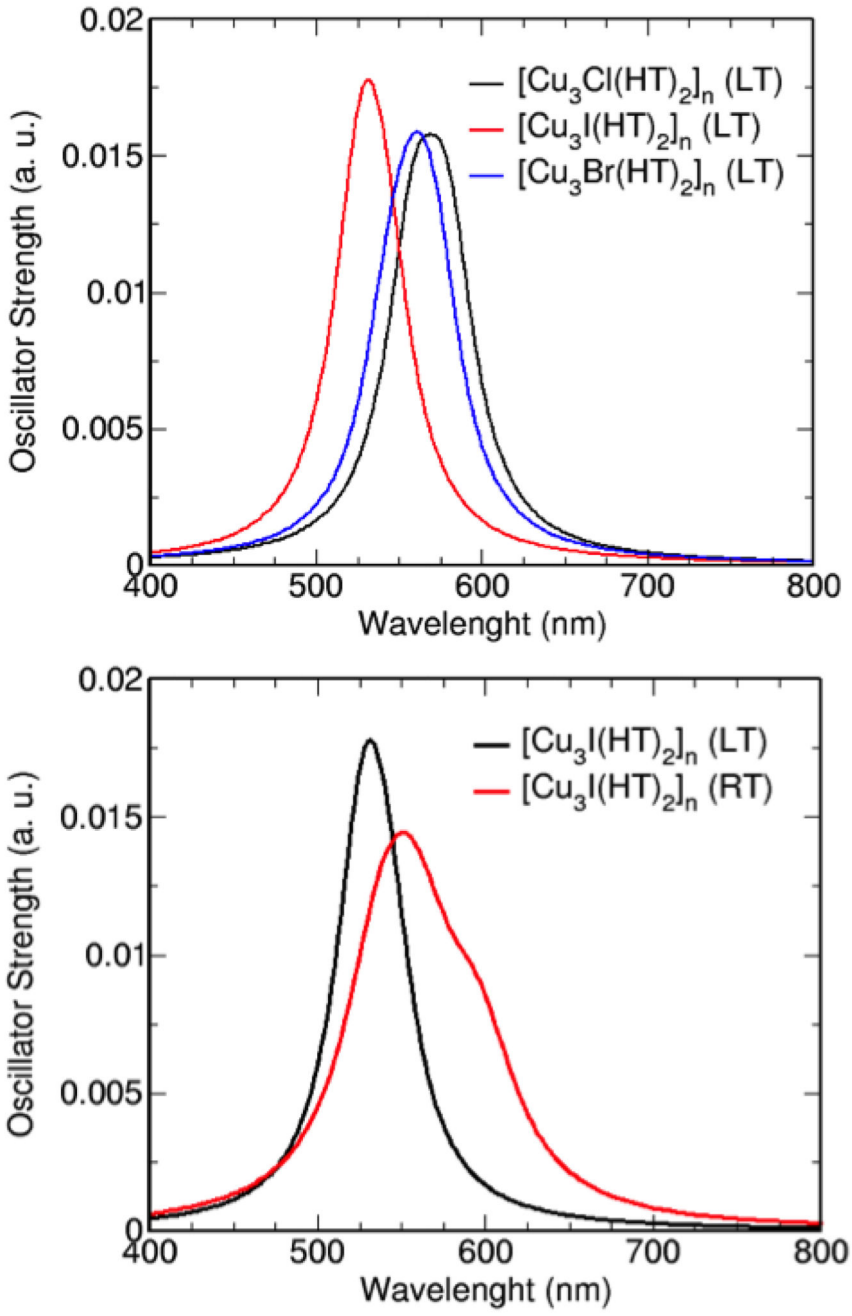

Figure 8.

Quasi-particle GW+BSE-corrected DFT excitation spectra for: (top) compounds **1**, **2** and **3** at *LT* conditions, and (bottom) compounds **3** and **3LT**.

Europe PMC Funders Author Manuscripts

Table 1

Deviation average values of the bond angles of the copper atoms regarding 120°, and distance of the copper atoms to the plane formed by sulfur and coordinated halides.

Compound		Average deviation 120-α (°)	Distance Cu-plane (Å)
1	Cu1	9.22	0.000
	Cu2	4.76	0.114
2	Cu1	10.86	0.029
	Cu2	6.77	0.217

Europe PMC Funders Author Manuscripts

Table 2

Excitation wavelengths and oscillator-strengths within the Quasi-particle GW+BSE corrected DFT formalism for the transitions VB-1/VB→CB/CB+1 excitations for **1**, **2**, **3** and **3LT**.

Transitions	Wavelenght (nm)	Oscillator Strength (a.u.)
Compound **1**		
VB-1→CB	560.5	0.0827
VB-1→CB+1	556.3	0.1032
VB→CB	576.8	0.0245
VB→CB+1	581.1	0.1847
Compound **2**		
VB-1→CB	554.8	0.0564
VB-1→CB+1	543.5	0.1438
VB→CB	565.5	0.0673
VB→CB+1	572.7	0.2742
Compound **3**		
VB-1→CB	538.9	0.0327
VB-1→CB+1	548.4	0.1465
VB→CB	568.2	0.0345
VB→CB+1	597.1	0.1041
Compound **3LT**		
VB-1→CB	530.6	0.0327
VB-1→CB+1	522.3	0.1132
VB→CB	543.5	0.0345
VB→CB+1	531.7	0.2247